

Monotonic and cyclic behavior of the nitrogen ion-implanted commercially pure-titanium

N. Ali^{1*}, M.S. Mustapa², T. Sujitno³, T.E. Putra¹, Husaini¹

¹ Department of Mechanical and Industrial Engineering, Faculty of Engineering, Universitas Syiah Kuala, Banda Aceh 23111, Indonesia
Phone: +62 8126906380

² Faculty of Mechanical and Manufacturing Engineering, Universiti Tun Hussein Onn Malaysia, 86400 Batu Pahat, Johor, Malaysia

³ National Nuclear Energy Agency of Indonesia, Jalan Babarsari PO Box 6101 Ykbb, Yogyakarta 55281, Indonesia

ABSTRACT – This research aims to study the behavior of monotonic and cyclic plastic deformation on commercially pure titanium which has undergone surface treatment using the nitrogen ion implantation method. The doses of 2.0×10^{17} ions/cm² and the energy of 100keV were used to implant the nitrogen ions into the CpTi. Monotonic properties tests were performed in a laboratory air and at room temperature using ASTM E8 standard specimens. Fatigue and corrosion fatigue tests were conducted in a laboratory air and in artificial saline solutions, at room temperature using ASTM 1801-97 specimens. Tensile tests were carried out with constant displacement rate and fatigue tests were carried under fully-reversed with stress-controlled conditions with stress amplitudes 230, 240, 250, 260, 270 and 280MPa. The results showed the material properties of monotonic behavior for CpTi and Nii-Ti; tensile strength (σ_u) of 497 and 539MPa and for 0.2% offset yield strength (σ_y) of 385 and 440MPa, respectively and of cyclic behavior; cyclic strength coefficient (k') of 568.41 and 818.64 and cyclic strain hardening exponent (n') of 0.176 and 0.215, respectively. This study has succeeded in producing useful new material properties that will contribute to the field of material science and engineering.

ARTICLE HISTORY

Received: 16th Apr 2020

Revised: 27th July 2020

Accepted: 22nd Aug 2020

KEYWORDS

Monotonic-cyclic behavior;
Ion implantation;
Cp-Ti fatigue;
corrosion-fatigue;
stress-cycle relationships

INTRODUCTION

Titanium and titanium alloys are included in the active metals group and have good corrosion resistance in saline environments. Additionally, titanium and its alloys have moderate mechanical properties and low density compared to steel and other non-steel metals [1]. With such properties, they are widely used as biomaterials in the form of implants [2]. Among them, commercially pure titanium (CpTi) is a very effective material for implants owing to its compatibility with body fluids and the fact that is non-toxic in the environment of the human body [3, 4]. When being used as a biomedical material, CpTi must have sufficient strength to tolerate daily activities. This is especially true for hip replacement surgeries, where the femoral head and metallic cup experience quite a lot of stress [4]. The rigidity of CpTi (160HV) [5] is relatively lower than that of stainless steel (180HV, ASTM/AISI A316) [6] which has also been used as a biomedical material. Therefore, it is necessary to treat the surface of CpTi that being applied for biomaterials for it to have adequate surface resistance.

Several methods of surface treatment and their effects on titanium have been reported by several researchers for the purpose of hardening of the material's surface [7]. The surface hardening techniques that were studied are treatment by anodic oxidation, sandblasting, coating by carbide, plasma nitriding, electrochemical treatment, laser treatment, solution treatment and nitrogen ion implantation [8-16]. Surface hardening through the ion implantation technique produces a hard surface without changing the dimensions and induces the surface hardness with a very thin case [17, 18]. The ion implantation technique uses nitrogen as an ion source and is expressed as CpTi [14]. Implantation of nitrogen ions produces a very hard titanium nitride phase (TiN and Ti₂N) on the CpTi surface [5].

The surface of CpTi will change some of the mechanical properties expressed by monotonic and cyclic behavior or fatigue. The cyclic behavior is known to cause fatigue in the laboratory environment, and in the corrosion media, it is known as corrosion fatigue. The properties of monotonic and cyclic behavior are expressed in the form of constants in the equations relating to static and dynamic behavior. A study by Branco *et al.* [19] has investigated the monotonic and cyclic behavior of the tempered alloy steel. Another related work is to study the estimation of the Basquin parameter, using high cycle fatigue test data [20]. So far, no paper has discussed the monotonic and cyclic behavior of nitrogen ion implanted CpTi.

Based on the description above, the monotonic and cyclic behavior of CpTi, which had undergone surface treatment using the nitrogen ion implantation method, is to be required as an effort to enrich the reference area. Therefore, the purpose of this study is to obtain the monotonic and cyclic properties of CpTi which has undergone surface treatments using the nitrogen ion implantation methods. The data presented in this study is important for developing and validating

more accurate analytical and numerical models, which can be used in the development of safer and more reliable mechanical and biomechanical components.

METHODS AND MATERIALS

Materials

The material used in this study was CpTi delivered from Fiko Ltd., Ukraine, in the form of a rod with a diameter of 30mm. CpTi-G2 has a moderate strength of these grades, with a minimum yield strength of 250MPa. It could be considered for any applications where biocompatibility, strength and corrosion resistance are important. It also has been shown to have good ductility, formability, and corrosion-fatigue resistance in seawater. The properties and compositions of the investigated materials are shown in Tables 1 and 2.

Table 1. Chemical composition of CpTi as delivered

Elements	N	C	H	Fe	O	Al	Si	Ti
Weight (%)	0.04	0.05	0.003	0.13	0.11	0.49	0.03	Base

Table 2. Mechanical properties of the CpTi as delivered

Tensile Strength (MPa)	Elongation (%)	Reduction Area (%)	Impact Strength
430	29	56	16

Process of Nitrogen Ions Implantation

In the ion implantation process, nitrogen ions are implanted into the surface of the components by using the kinetic energy of high beam energy, so that the ions penetrate the crystal structures [21]. As a result, the surface is geometrically almost unchanged but contains an extremely fine dispersion of titanium nitrides. The hard nitride phases improve the tribological properties by increasing surface hardness and reducing abrasion [18].

The implantation of the nitrogen ions into the CpTi surface was performed in a target chamber of the particles accelerator (Type: Cockcroft-Walton; model: ICS-SP 1104 200keV/ 200μA) in the Center for Accelerator Technology at Badan Tenaga Atom Nasional (BATAN), Yogyakarta, Indonesia. The vacuum of the target chamber was maintained below 10^{-6} mBar, during the ion implantation process. The current density of the ion beam was maintained between 50 and 200μA/cm². The ion beam processes operate at a temperature between 150°C and 200°C, depending on the level of the ion beam flux, [22]. The parameter used for the implantation of nitrogen ion was with the doses of 2.0×10^{17} ions/cm² and the energy of 100 keV. The dose of 2.0×10^{17} ions/cm² and energy of 100keV were a combination of ions implantation parameters that obtained optimal CpTi surface properties as stated in previous studies by Fulazzaky [5].

Monotonic Stress-Strain Test

A Shimadzu Servopulser, a universal testing machine, was used to measure the tensile stress of CpTi and Nitrogen implanted CpTi (Nii-Ti). The tensile testing machine used was connected to a computer and was run through a specialized software (Shimadzu Gluon, Version 2.40). The specimen and procedure used followed ASTM E 8 - 08 standard [23]. Two specimens with a diameter of 6 mm were tested at room temperature and at displacement rate of 1 mm per minute until the specimen fracture occurred. Figure 1 shows the tensile test specimen according to ASTM E-8. The engineering stress and strain, shown in this paper as σ and ϵ , respectively, were determined from the maximum load using the original cross-sectional area of the specimen. The strain was computed using a gauge length of the specimen as referred to in the work of Ali et al. [24]. The engineering stress and strain are defined by the ratio of maximum tensile load and original area and the total elongation and original gauge length, respectively [25].

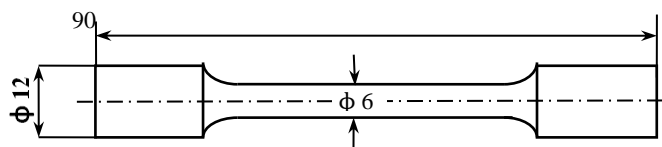


Figure 1. Shape and size of the tensile test specimen (in mm)

Fatigue Test

The stress-amplitude controlled fatigue tests were conducted (fully-reversed loading) using Shimadzu Servopulser 100 kN capacity. Shimadzu Gluon test execution and data processing software version 2.40: 2001 were used to run the fatigue test and data processing. Axial stresses are applied in the range of 20% - 50% under tensile stress (the stress amplitude lies between 230–320MPa) [26] with the stress ratio $R=-1$ and frequency 10-20Hz. Three charges of the specimen were prepared to achieve the behavior of fatigue in an air laboratory environment and in a saline solution which is defined as corrosion fatigue. The fatigue testing of two charge specimens CpTi and nitrogen ion implanted-titanium (Nii-Ti) was carried out in an air laboratory environment and the other charge of the specimen (Nii-Ti) was tested in a saline solution. The corrosion chamber was attached to the gage section using the same silicone adhesive. The form and size of the specimen used are shown in Figure 2 according to the ASTM 1801-97 [27].

The gage section of the specimen for corrosion fatigue testing was submerged in the saline solution using a corrosion chamber; a fluid supply system and saline solution in a reservoir during fatigue testing. The fatigue tests were carried out on the original CpTi specimens and the nitrogen implanted CpTi specimens, while corrosion fatigue tests were carried out on nitrogen ion implanted CpTi specimens. The corrosion fatigue properties of CpTi has been studied by Zavanelli [28] in terms of corrosion fatigue life for a selected stress level. A pump was utilized to provide a fresh supply of corrosive fluid to the specimen with a flow rate of 500ml/min. An air compressor was also used to supply oxygen to the fluid reservoir through a diffuser ball. This action would provide constant oxygen content in the solution during the fatigue test. The saline solution is prepared as a corrosion medium according to ASTM F1801-97 [27]. Figure 3 shows the Shimadzu Servopulser 100kN fatigue machine running a test.

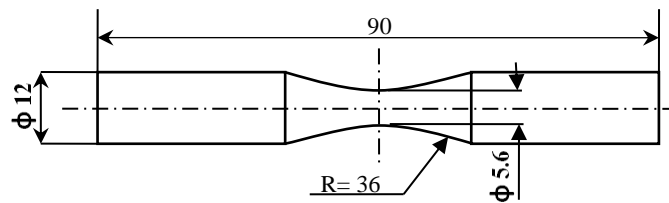


Figure 2. Form and size of the fatigue specimen (in mm).

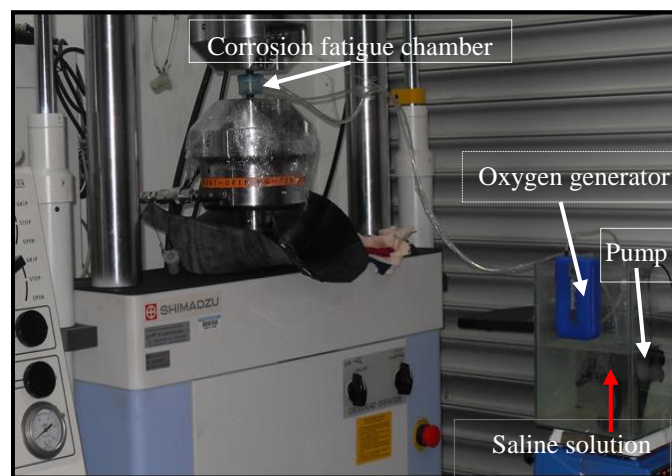


Figure 3. Fatigue tests machine of the Shimadzu Servopulser 100kN capacity

RESULTS AND DISCUSSION

Monotonic Stress-Strain Relationship

The presence of nitrides phase on a nitrogen ions implanted surface caused a change of the tensile properties of the CpTi. The change in tensile property is significant, data from experimental work verifies that the maximum tensile stress value is 539MPa for nitrogen-ions implanted CpTi. Therefore, Nii-Ti is stronger than that of 497MPa for the CpTi in σ_u - ϵ stated in the σ_u - ϵ graph as shown in Figure 4. The effect of nitrogen ion implantation is clarified with the increasing of the tensile properties of the CpTi surface. This is due to the presence of foreign atoms inside the substrate, besides surface damage and lattices defect, which changes the configuration of the microstructure on the material [29].

The change in strain is quite significant, experimental data verifies that the maximum ϵ value of 0.367 (or 36.7%) for Nii-Ti in σ_u - ϵ is more ductile than that of 0.333 (or 33.3%) for CpTi in σ_u - ϵ , as shown in Figure 4. The value of ϵ for Nii-Ti is more ductile than those of CpTi due to the possible crystal lattice structures of Ti atoms that have reacted with

nitrogen to form more flexible amorphous structures of the titanium nitride (TiN) phase at the implanted CpTi surface. Figure 4 shows the engineering stress-strain graph of CpTi and Nii-Ti. Figure 5 shows the true stress-strain graph of CpTi and Nii-Ti. The improvement of tensile stress and elongation of Nii-Ti specimens is due to the formation of a new phase composed of a mixture of face-centered cubic (fcc) TiN and tetragonal Ti₂N which inhibits further nitrogen diffusion into the bulk [30]. It was concluded that the mechanical properties of Nii-Ti are quite different from the CpTi specimen.

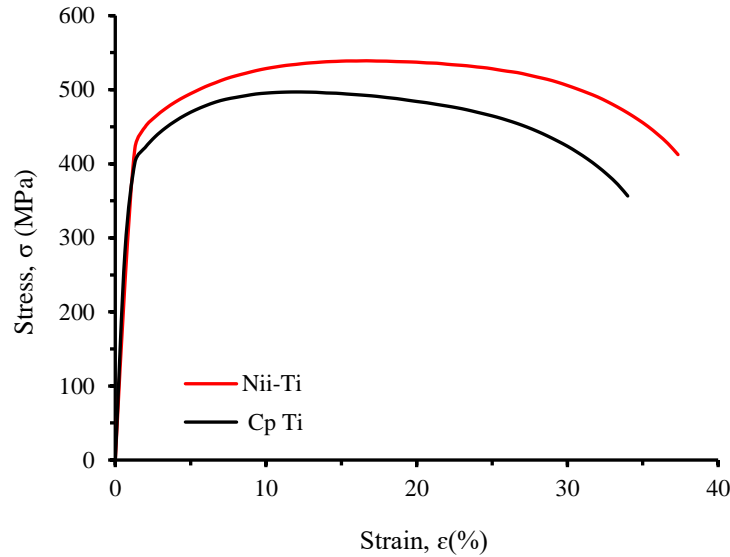


Figure 4. Engineering stress-strain curve of CpTi and Nii-Ti

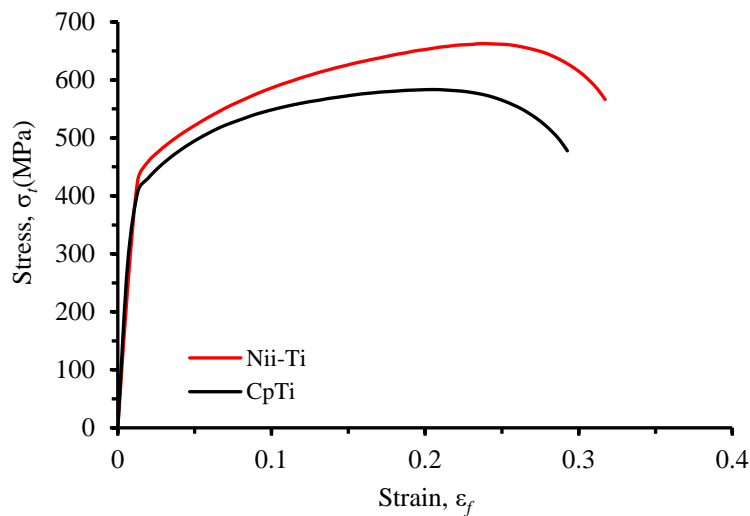


Figure 5. True stress-strain curve of CpTi and Nii-Ti

Offset Yield Strength of CpTi and Nii-Ti

The calculation of 0.2% offset yield strength is subjected to verify the yield strength of used materials in the current study. The procedure of measurement is referred to as ASTM E8-04 [23]. The results of tensile properties are shown in Table 3. The mechanical properties shown in Table 3 are the verification results for the graphs in Figures 4 and 5. The tensile properties of CpTi are 497MPa and 385MPa for tensile and yield stress, respectively, while for Nii-Ti are of 539MPa and 440MPa.

Table 3. Mechanical properties of CpTi and Nii-Ti

Parameter	Symbol (Unit)	Specimen	
		CpTi	Nii-Ti
Young Modulus	E (GPa)	100	100
Ultimate tensile strength	σ_u (MPa)	497	539
Yield stress (0.2% offset)	σ_y (MPa)	385	440
Elongation (25 mm)	(%)	33.3	36.7
True fracture strength	σ_f (MPa)	703.63	718.72
True fracture ductility	-	0.429	0.457

The total true strain is defined as the summation of elastic and plastic components that can be expressed in an Eq. (1):

$$\epsilon_t = \epsilon_e + \epsilon_p \tag{1}$$

The true stress versus true plastic strain plot is modeled as a straight line. The curve is expressed using a power law function as in Eq. (2):

$$\sigma_f = k(\epsilon_p)^n \tag{2}$$

where σ_t represents the true stress of the material, ϵ_p is the true strain, k is the strength coefficient and n is strain hardening exponent. The strain hardening exponent value ranges between 0 and 1. The zero value (0) identifies that a material is a perfect plastic solid, while the value 1 represents a 100% elastic solid. Most metals have n values between 0.1 and 0.5. [31].

Two important quantities can be defined at the fracture of the tensile test. These are true fracture strength (σ_f is true stress at final fracture) and true fracture ductility as shown in Eq. (3):

$$\sigma_f = \frac{P_f}{A_f} \tag{3}$$

where A_f donated the area at fracture and P_f donated the load at fracture. Eq.s (4) and (5) show the fracture ductility:

$$\epsilon_f = \ln \frac{A_0}{A_f} = \ln \frac{1}{1 - RA} \tag{4}$$

$$RA = \frac{A_0 - A_f}{A_0} \tag{5}$$

where RA is the reduction area

The true fracture properties of CpTi and Nii-Ti are summarized in Table 4. The value of the true fracture properties involves true strength (σ_f), true strain (ϵ_f) and Reduction Area (RA).

Table 4. The value of true fracture properties

Sample	P_f (N)	A_f (mm ²)	σ_f (Mpa)	A_0 (mm ²)	RA	ϵ_f
CpTi	477	3.86	703.63	5.93	0.349073	0.429357
Nii-Ti	566	3.76	718.72	5.94	0.367003	0.457290

The strength coefficient is defined, k in term of true stress at facture, σ_f and the true strain ϵ_f ; as shown in Eqs. (6) and (7):

$$\sigma_f = k(\epsilon_f)^n \tag{6}$$

and

$$k = \frac{\sigma_f}{\epsilon_f^n} \tag{7}$$

Log-log plot of the true stress and true strain resulting in the value of strength coefficient (k) and strain hardening exponent (n) is shown in Figure 6. Table 5 summaries the value of strength coefficient (k) of 933 and 1133 MPa and for CpTi and Nii-Ti and the value strain hardening exponent (n) of 0.21 and 0.26 for CpTi and Nii-Ti, respectively.

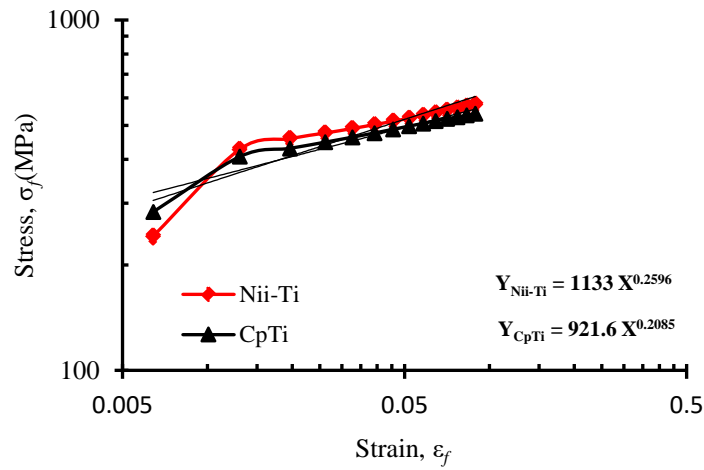


Figure 6. The plot of true stress vs true strain for CpTi and Nii-Ti

Table 5. The strength coefficient (*k*) and strain hardening exponent (*n*)

Sample	<i>k</i> (MPa)	<i>n</i>
CpTi	922	0.21
Nii-Ti	1133	0.26

The obtained curve as shown in Figure 5 can be described by the power law formula as follow, Eq. (8):

$$\sigma_f = 922(\varepsilon_f)^{0.21} \text{ for CpTi}$$

(8)

$$\sigma_f = 1133(\varepsilon_f)^{0.26} \text{ for Nii - Ti}$$

Cyclic Stress-Strain Relationships

The stress-plastic strain power law relation for fatigue CpTi and Nii-Ti is described in Eq. (9):

$$S_a = k'(\varepsilon_p)^{n'}$$

(9)

where S_a is the stress amplitude (MPa), ε_p is the plastic strain, k' (mm/mm) is the strength coefficient and n' is cyclic strain hardening exponent. Tables 6 and 7 show the data of cyclic strain vary with stress amplitude for CpTi and Nii-Ti, while Figure 7 and Figure 8 draw the log-log plot of stress amplitude and plastic strain for CpTi and Nii-Ti. The standard value of strain hardening exponent lies between 0.10 and 0.25 [31].

Table 6. The variation of cyclic strain with stress amplitude for CpTi

Stress amplitude (S_a , MPa)	Plastic strain (ε_p)	Elastic strain (ε_e)
230	0.0062	0.3261
240	0.0064	0.3647
250	0.0087	0.3665
260	0.0148	0.3924
270	0.0136	0.4574
280	0.0127	0.4610

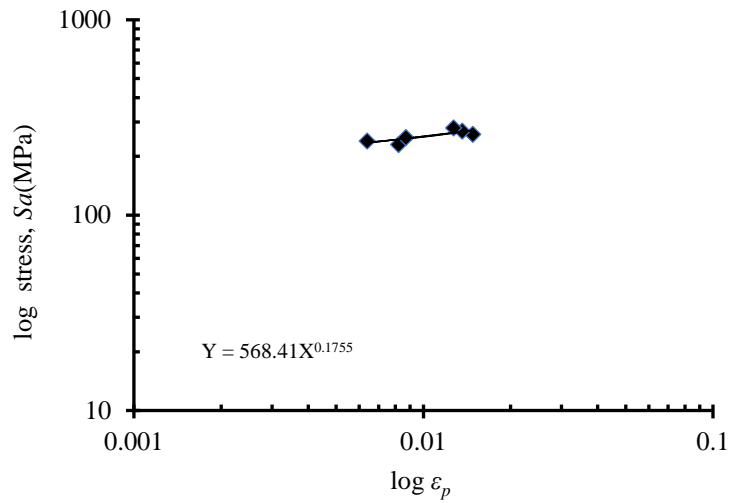


Figure 7. The true stress amplitude vs true plastic strain plot of CpTi

Table 7. The variation of cyclic strain with stress amplitude for Nii-Ti

Stress amplitude (S_a, MPa)	Elastic strain (ϵ_e)	Plastic strain (ϵ_p)
260	0.3683	0.0043
270	0.4034	0.0069
280	0.4200	0.0086
300	0.4291	0.0082
320	0.4156	0.0102

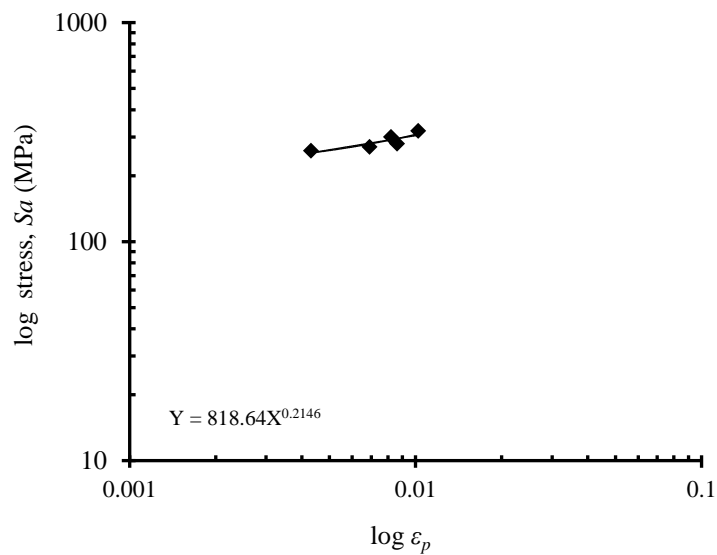


Figure 8. The stress amplitude vs true plastic strain plot of Nii-Ti

Table 8. The values of cyclic strength coefficient (k') and strain hardening exponent (n')

Sample	k' (MPa)	n'
CpTi	568.41	0.176
Nii-Ti	818.64	0.215

The value of k and n' for CpTi and Nii-Ti are established from power function as shown in Eq. (9), described from the plot in Figures 6 and 7 and summarized in Table 8. The value of k' is 568.14 and 818.64 for CpTi and Nii-Ti and the value n' is 0.176 and 0.215 for CpTi and Nii-Ti, respectively. The value k' and n' are then substituted into Eq. (9), then the result in Eq. (10):

$$S_a = 568.41(\epsilon_p)^{0.176} \text{ for Cp-Ti} \tag{9}$$

and

$$S_a = 818.64 (\epsilon_p)^{0.215} \text{ for Nii-Ti} \tag{10}$$

The results of n' values for both specimens are following the standard value and agree with the work of Kosturek et al. [32]. Regression analysis results found that the value of R^2 is below 0.8, however, the values of strain hardening exponent (n') were still within the standard range. Therefore, the results obtained in this study are still acceptable with a few notes. This is because of the use of very limited data to draw the graphs (ref. to Figures 7 and 8).

Formulation of Stress-Cycle Relationships

The stress-life method is a classic method for analyzing metal fatigue and this method was originally the result of Wöhler's work in 1860. The strength in the structure or component of the machine is related to the limit of material fatigue. The basis of this method is the S-N curve of the material obtained by testing it in the laboratory for small specimens until the material fails. The S-N behaviors of CpTi and Nii-Ti in laboratory air and in saline solution follows Wöhler's linear relationships in comparison with the work of Fleck & Eifler [33]. Figure 9 shows the Semi-log plot of the S-N curve that can be achieved the Wöhler's and Busquin's relationships. The Wöhler equation is obtained by formulating the linear relationship of the S-N curve for CpTi, Nii-Ti in the air laboratory and Nii-Ti in saline solution, corrosion fatigue, (refer to Figure 9) respectively, as shown in Eq. (11).

$$\begin{aligned} S_a &= 290.77 - 5.0 \times 10^{-6}(N_f); \text{ for CPTi,} \\ S_a &= 293.81 - 4.0 \times 10^{-6}(N_f); \text{ for Nii-Ti,} \\ S_a &= 292.19 - 1.0 \times 10^{-5}(N_f); \text{ for Nii-Ti in saline solution, and} \\ S_a &= 291.19 - 1.0 \times 10^{-4}(N_f); \text{ Fleck \& Eifler [33]} \end{aligned} \tag{11}$$

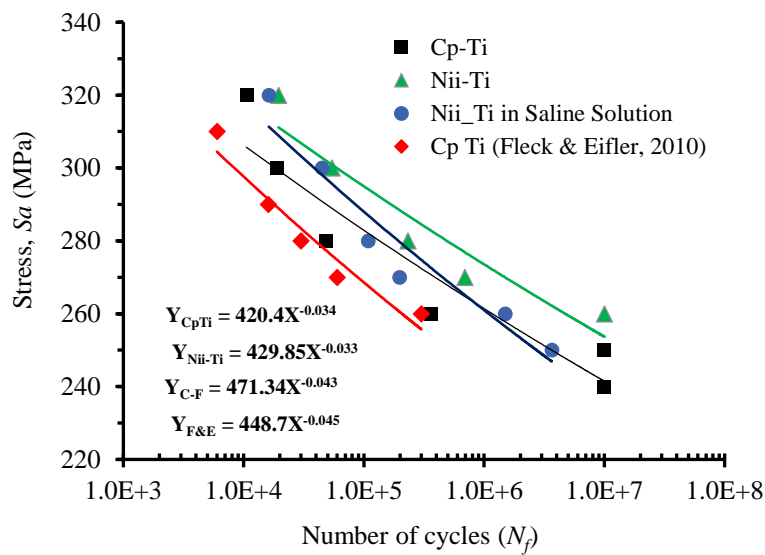


Figure 9. Relationships of semi-log S-N curve for obtaining the Wöhler's and Busquin's formula

The following equations identifies the Busquin's formula for CpTi, Nii-Ti in air laboratory and Nii-Ti in saline solution, respectively:

$$\begin{aligned} S_a &= 420.40(N_f)^{-0.034}, \text{ for CpTi,} \\ S_a &= 429.85(N_f)^{-0.033}, \text{ for Nii-Ti, and} \\ S_a &= 471.34(N_f)^{-0.043}, \text{ for Nii-Ti in saline solution} \\ S_a &= 448.70(N_f)^{-0.045}, \text{ Fleck \& Eifler [33]} \end{aligned} \tag{12}$$

Eq. (12) is in accordance with the Basquin's law that is the change in fatigue life, N_f , with stress amplitude, S_a [20]:

$$S_a = \frac{\Delta S}{2} = S'_f (N_f)^b \quad (13)$$

or

$$\frac{\Delta \varepsilon_e}{2} = \frac{S}{2E} = \frac{S'_f}{E} (N_f)^b \quad (14)$$

where, S'_f represents the coefficient of fatigue strength and b represents the elastic exponent also known as the Basquin's exponent. The value of S'_f and b is listed in Table 9. From Table 9 can be seen that b values for all specimens lies between -0.33 and -0.43. These values are slightly smaller than the standard values for metals, which range from ≈ 0.05 to -0.12, with standard deviations above 90%. This result is therefore very acceptable as valid data.

Table 9. Coefficient of fatigue strength (S'_f) and elastic exponent (b)

Sample	S'_f (MPa)	b	R^2
CpTi	420.40	-0.034	0.90
Nii-Ti	429.85	-0.033	0.91
Nii-Ti in Soline Solution	471.34	-0.043	0.93
Cp-Ti Fleck & Eifler [33]	448.70	-0.040	0.94

CONCLUSIONS

This study provides useful information regarding material properties that will contribute to the fields of materials science and technology. The monotonic properties for CpTi and Nii-Ti were tensile strength (σ_u) of 497MPa and 539 MPa and 0.2% offset yield strength (σ_y) of 385 and 440MPa, respectively and the strength coefficient (k) of 922 and 1133MPa and strain hardening exponent (n) of 0.21 and 0.26, respectively. The cyclic properties were the stress amplitude of 250MPa for CpTi and the stress amplitude of 260MPa for Nii-Ti cyclic strength coefficient (k') of 568.41 and 818.64MPa and cyclic strain hardening exponent (n') of 0.176 and 0.215, respectively.

ACKNOWLEDGMENTS

The authors would like to acknowledge the Ministry of Science, Technology and Innovation, Malaysia (Science Fund, Vot. S015) and Universitas Syiah Kuala (Contract Number: 289 / UN11 / PSP / PNB / 2018, PCP) for research grants and funding.

REFERENCES

- [1] H. Kaminaka, M. Abe, S. Matsumoto, K. Kimura, H. Kamio, "Characteristics and Applications of High Corrosion Resistant Titanium Alloys," *Nippon Steel & Sumitomo Metal Technical Report* vol. 106, pp. 34-40, 2014.
- [2] R. P. Nitesh, P. G. Piyush, "A Review on Biomaterials: Scope, Applications & Human Anatomy Significance," *International Journal of Emerging Technology and Advanced Engineering*, vol. 2, pp. 91-101, 2012.
- [3] N. Azida, C. Lah, M. H. Hussin, "Titanium and Titanium Based Alloys as Metallic Biomaterials in Medical Applications – Spine Implant Case Study," *Pertanika Journal Science & Technology* vol. 27, pp. 459 - 472, 2019.
- [4] M. Niinomi, M. Nakai, "Titanium-based biomaterials for preventing stress shielding between implant devices and bone," *International Journal of Biomaterials*, vol. 2011, pp. 1-10, 2011.
- [5] M. A. Fulazzaky, N. Ali, H. Samekto, M. I. Ghazali, "Assessment of CpTi Surface Properties after Nitrogen Ion Implantation with Various Doses and Energies," *Metalurgical and Materials Transactions A*, vol. 43A, pp. 4185-4193, 2012.
- [6] ASM, *Metals Handbook*, 10 ed. vol. 1. OH: ASM International Materials Park, 1990.
- [7] A. Jemat, M. J. Ghazali, M. Razali, Y. Otsuka, "Surface Modifications and Their Effects on Titanium Dental Implants," *BioMed Research International*, vol. 2015, pp. 1-11, 2015.
- [8] D. Velten, V. Biehl, F. Aubertin, B. Valeske, W. Possart, J. Brems, "Preparation of TiO₂ layers on cp-Ti and Ti6Al4V by thermal and anodic oxidation and by sol-gel coating techniques and their characterization," *Journal Biomedical Materials Research*, vol. A59, pp. 18-28, 2002.
- [9] M. P. Kapczinski, C. Carlos Gil, E. J. Kinast, C. Alberto dos Santos, "Surface modification of titanium by plasma nitriding," *Materials Research*, vol. 6, pp. 265-271, 2003.

- [10] A. S. Guilherme, "Surface roughness and fatigue performance of commercially pure titanium and Ti-6Al-4V alloy after different polishing protocols," *The Journal of Prosthesis Dental* vol. 93, pp. 378 - 385, 2005.
- [11] J. Jagielski, A. Piatkowska, P. Aubert, L. Thome, A. Turos, A. Abdul Kader, "Ion implantation for surface modification of biomaterials," *Surface & Coatings Technology*, vol. 200, pp. 6355-6361, 2002.
- [12] X. P. Jiang, X. Y. Wang, J. X. Li, C.-S. Man, M. Shepard, T. Zhai, "Enhancement of fatigue and corrosion properties of pure Ti by sandblasting.," *Materials Science and Engineering A*, vol. A429, pp. 30-35, 2006.
- [13] H.-J. Song, M.-K. Kim, G.-C. Jung, M.-S. Vang, Y.-J. T. S. C. T. Park, pp. 8738-8745., "The effect of spark anodizing treatment of pure titanium metals and titanium alloys on corrosion characteristics," *Surface & Coating Technology*, vol. 201, pp. 8738-45, 2007.
- [14] N. Ali, H. Samekto, M. I. Ghazali, M. Ridha, "Surface Modification of Pure Titanium by Nitrogen Ion Implantation at Different Beam Energy and Dose," *Key Engineering Materials*, vol. 462-462, pp. 750-755, 2011.
- [15] A. N. Nassier, D. Robert Birch, S. P. Rico Sierra, G. Edwardson, Z. G. Dearden, "Surface Modification of Titanium Alloy with Laser Treatment," *International Journal of Aerospace and Mechanical Engineering*, vol. 12, pp. 580-583, 2018.
- [16] Alfrano, S. S. Friandani, C. Sutowo, "Effect of solution treatment on the microstructure and mechanical properties of Ti-6Al-6Mo hot-rolled alloy," *Journal of Mechanical Engineering and Sciences*, vol. 13, pp. 4857-4868, 2019.
- [17] J. Jin, W. Wang, X. Xinchun, "Microstructure and Mechanical Properties of Ti + N Ion Implanted Cronidur30 Steel," *Materials*, vol. 12, pp. 427-439, 2019.
- [18] Sudjatmoko, R. M. Lely Susita, Wirjoadi, B. Siswanto, "Effects of Nitrogen Ion Implantaion on Hardness and Wear Resistance of the Ti-6Al-4V alloy," *Jurnal Iptek Nuklir Ganendra* vol. 18, pp. 61-68, 2015.
- [19] R. Branco, J. D. M. Costa, F. V. Antunes, S. Perdigão, "Monotonic and Cyclic Behavior of DIN 34CrNiMo6 Tempered Alloy Steel," *Metals*, vol. 6, pp. 1-14, 2010.
- [20] H. Özdeş, M. Tiryakioğlu, "On Estimating High-Cycle Fatigue Life of Cast Al-Si-Mg-(Cu) Alloys from Tensile Test Results," *Material Science and Engineering A*, vol. 688, pp. 9-15, 2017.
- [21] T. R. Rautray, R. Narayanan, K.-H. Kim, "Ion implantation of titanium based biomaterials," *Progress in Materials Science*, vol. 56, pp. 1137-1177, 2011.
- [22] E. Woolley, "Surface hardening by ion implantation," *Materials World*, vol. 5, pp. 515-516, 1997.
- [23] ASTM and Standard, "Standard Test Methods for Tension Testing of Metallic Materials," in *Annual Book of ASTM Standards*. vol. 01: ASTM International, 2008, pp. 1-24.
- [24] N. Ali, M. A. Fulazzaky, M. S. Mustapa, M. I. Ghazali, M. Ridha, T. Sujitno, "Assessment of fatigue and corrosion fatigue behaviours of the nitrogen ion implanted CpTi " *International Journal of Fatigue* vol. 61, pp. 184-190, 2014.
- [25] J. A. Bannantine, J. J. Comer, J. L. Handrock, *Fundamentals of Metal Fatigue Analysis 1st Edition*, 1 ed. Englewood Cliffs, NJ: Prentice Hall, 1990.
- [26] A. Lipski, "Determination of the S-N Curve and the Fatigue Limit by Means of the Thermographic Method for Ductile Cast Iron," 2018, pp. 020008-1-020008-8.
- [27] ASTM and Standard, "Standard Practice for Corrosion Fatigue Testing of Metallic Implant Materials," in *Annual Book of ASTM Standard, ASTM F1801-97*: ASTM International, 2008.
- [28] R. A. Zavanelli, E. P. H. Guilherme, I. Ferreira, J. M. D. de Alamida Rollo, "Corrosion-fatigue life of commercially pure titanium and Ti-6Al-4V alloy in differenct storage environments," *Journal of Prosthetic Dentistry*, vol. 84, pp. 274-279, 2000.
- [29] F. L. Wen, Y.-L. Lo, "Surface Modification of SKD-61 steel by ion implantation technique," *Journal of Vacuum Science and Technology*, vol. 25, pp. 1137-1142, 2007.
- [30] G. Cassar, S. Banfield, J. C. Avelar-Batista Wilson, J. Housden, A. Matthews, A. Layland, "Impact wear resistance of plasma diffusion treated and duplex treated/PVD-coated of Ti-6Al-4V alloy," *Surface and Coating Technology*, vol. 206, pp. 2645-54, 2012.
- [31] R. L. Stephens, A. Fatemi, R. R. Stephens, H. O. Fuchs, *Metal Fatigue in Engineering*, 2 ed. New York: Jonh Wiley & Sons inc, 2001.
- [32] R. Kosturek, L. Sniezek, J. Torzewski, M. Wachowski, "Low Cycle Fatigue Properties of Sc-Modified AA2519-T62 Extrusion," *Materials* vol. 13, pp. 1-12, 2020.
- [33] C. Fleck, D. Eifler, "Corrosion, fatigue and corrosion fatigue behaviour of metal implant materials, especially titanium alloys," *International Journal of Fatigue*, vol. 32, pp. 929-935, 2010.